

A unified quantile framework reveals nonlinear heterogeneous transcriptome-wide associations

Tianying Wang*

Department of Statistics, Colorado State University

Iuliana Ionita-Laza and Ying Wei

Department of Biostatistics, Columbia University

August 23, 2023

Abstract

Transcriptome-wide association studies (TWAS) are powerful tools for identifying putative causal genes by integrating genome-wide association studies and gene expression data. However, most TWAS methods focus on linear associations between genes and traits, ignoring the complex nonlinear relationships that exist in biological systems. To address this limitation, we propose a novel quantile transcriptomics framework, QTWAS, that takes into account the nonlinear and heterogeneous nature of gene-trait associations. Our approach integrates a quantile-based gene expression model into the TWAS model, which allows for the discovery of nonlinear and heterogeneous gene-trait associations. By conducting comprehensive simulations and examining various psychiatric and neurodegenerative traits, we demonstrate that the proposed model outperforms traditional techniques in identifying gene-trait associations. Additionally, QTWAS can uncover important insights into nonlinear relationships between gene expression levels and phenotypes, complementing traditional TWAS approaches. We further show applications to 100 continuous traits from the UK Biobank and 10 binary traits related to brain disorders.

Keywords: Regression quantile process; Nonlinear association test; Transcriptome-Wide Association Studies.

*T.W. thanks for support from the National Natural Science Foundation of China (Grant No. 12101351). Y. W. thanks for support from the National Institutes of Health (HG008980 and 1RF1AG072272) and the National Science Foundation (DMS-1953527). I. I.-L. thanks for support from the National Institutes of Health (GM143298, HG012345, AG072272, and MH095797).

1 Introduction

Genome-wide association studies (GWAS) play a central role in identifying genotype-phenotype relationships and can provide important insights into the etiology of complex traits and guide the development of targeted therapeutic strategies. Over the past fifteen years, GWAS have been widely conducted and successfully identified tens of thousands of genetic variants, specifically single nucleotide polymorphisms (SNPs) associated with various complex diseases and traits. Since it is assumed that most functional genetic variants exert their effects on traits or diseases through their influence on gene expression, directly linking gene expression levels to traits or diseases can provide a better understanding of the underlying biological mechanisms (Li et al., 2021; Tang et al., 2021; Li et al., 2021), and facilitates the identification of potential therapeutic targets. The main challenge to such studies is that gene expression levels are not easily available in large-scale studies, and therefore approaches have been developed to impute gene expression levels based on DNA sequence data. One recent approach along this line has been proposed, namely the transcriptome-wide association studies (TWAS) (Gusev et al., 2016; Gamazon et al., 2015; Zhao et al., 2021; Xie, Shan, Zhao, and Hou, Xie et al.; Wainberg et al., 2019). TWAS starts with the incorporation of large-scale data on both genotype and gene expression as available in projects such as the Genotype-Tissue Expression (GTEx) project (GTEx Consortium et al., 2015; GTEx Consortium, 2020), which provides information on the transcriptional regulation across various human tissues.

More specifically, TWAS is an integrative analysis that combines two distinct models – a gene expression model (Model A in Figure 1) that models gene expression as a function of expression quantitative trait loci (eQTLs, i.e., genetic variants that are associated with gene expression), and a GWAS model (Model B in Figure 1) that captures the associations

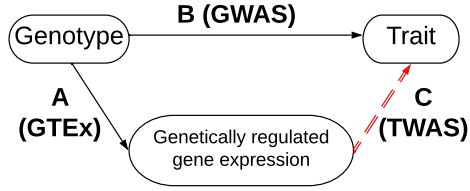


Figure 1: Quantile TWAS and classical linear TWAS models. Model A: a model for SNP-gene expression association (eQTL model based on GTEx data). Model B: a model for SNP-Trait associations (GWAS model). Model C: a model for expression-trait association (TWAS model).

between a trait and individual genetic variants. The two models are estimated separately and then combined to infer associations between genetically regulated gene expression levels and phenotypes (i.e., TWAS, represented by Model C in Figure 1). For example, the widely-used PrediXcan (Gamazon et al., 2015) first uses a sparse linear model such as elastic net or lasso to estimate the cis-eQTL effects on gene expression and then imputes gene expression levels. Then, in the second step, it formally tests the association between imputed gene expression (genetically regulated gene expression levels) and the trait of interest. S-PrediXcan (Barbeira et al., 2018) expands its application by only requiring GWAS summary statistics instead of individual-level data, which are not easily available due to privacy issues. Similarly, Gusev et al. (2016) and Nagpal et al. (2019) considered Bayesian gene expression models (Model A) instead of simple linear models in their TWAS approaches. To leverage multi-tissue data, UTMOST (Hu et al., 2019) proposed a multi-task learning method to jointly model gene expression across tissues and then integrate them into an overarching gene-trait association test.

Current TWAS methodologies rely on the premise that both gene expression models (Model A, SNP-gene expression association) and the GWAS model (Model B, SNP-trait as-

sociation) are linear. However, multiple lines of evidence suggest substantial heterogeneity in gene expression patterns caused by genetic variations, cellular and molecular heterogeneity along with environmental, demographic, and technical factors (Leek and Storey, 2007; Somel et al., 2006; Budinska et al., 2013). Similarly, several studies such as Umans et al. (2021) found that the regulation of gene expression through eQTLs can be context-dependent and highly influenced by gene-gene and gene-environment interactions (GEI). Wang et al. (2019) searched for eQTLs associated with the variance of gene expression levels and showed that they are enriched in GEI effects, suggesting that heterogeneous associations may result from widespread GEI. More recently, Lin et al. (2022) reported new TWAS discoveries by examining quadratic gene expression models. In summary, previous studies in the literature suggest that modeling nonlinear heterogeneous associations can be important for improving the accuracy of gene expression prediction models and improving the power of TWAS approaches (Song et al., 2017; Wang et al., 2023).

The Quantile TWAS (QTWAS) framework we propose here offers a means to implement such nonlinear transcriptome-wide associations. Our methodology involves a two-stage process. First, we employ quantile regression paired with a quantile-specific variable screening scheme to model the conditional distribution of gene expression based on the genotype data. Second, through the integration of the distribution-wise imputed gene expression and GWAS summary statistics, we are able to identify nonlinear TWAS associations (Model C in Figure 1). Modeling the complete conditional distribution of gene expression given genetic variants makes our methodology different from existing ones. Another key innovation lies in the unique integration of the conditional distribution of gene expression with GWAS summary statistics to infer nonlinear gene-trait associations. We establish an appropriate theoretical framework and rigorous statistical inference tools.

We applied QTWAS to investigate transcriptome-wide associations of protein-coding genes with their gene expression levels in whole blood tissue in GTEx (v8) (GTEx Consortium, 2020), and published GWAS summary statistics from 100 continuous phenotypes in UK Biobank and 10 psychiatric and neurodegenerative disorders.

2 Methodology

2.1 Notations and background

In this paper, we use X to represent the gene expression level of a target gene, Y for a trait/phenotype, and $Z = (Z_1, \dots, Z_p)^\top$ to denote a vector of p genetic variants. We assume Y is continuous and will extend the QTWAS method into binary traits later. SNPs Z_1, \dots, Z_p are discrete random variables with possible values of 0, 1, 2, signifying the number of reference alleles at a locus. As with other TWAS methods, we focus on SNPs (Z) located within $\pm 1\text{Mb}$ from the target gene, as such regions encompass most of the identified eQTLs for a gene (GTEx Consortium, 2020). Possible confounders in genetic association studies include race and ethnicity, principal components (PCs) of genotype data, and probabilistic estimation of expression residuals (PEER) factors are normally used as covariates in linear regression models to remove their effects (Stegle et al., 2012; Hu et al., 2019; Stegle et al., 2010). Without loss of generality, we assume that these confounding effects on phenotypes Y and gene expression X have been removed. Further, we use C to represent other covariates that are uncorrelated to Z , such as age, gender, and other postnatal nongenetic factors.

TWAS aims to identify genes whose expression levels (X) are associated with an out-

come of interest (Y). A simple linear regression model is often assumed:

$$\text{GeneExpression} - \text{Trait (Model C)} : Y = \alpha_{0,y} + \gamma X + C^\top \alpha_y + \epsilon_y, \quad (1)$$

where $\alpha_{0,y}$ is the intercept; γ and α_y are coefficients corresponding to X and C , respectively; ϵ_y is the random error with mean zero. The goal of TWAS is to test $H_0 : \gamma = 0$. Ideally, we would need data where both gene expression and phenotype are available. However, in many cases, gene expression data are not available for the relevant tissues or conditions, or the sample size may be too small to detect significant associations. Instead, TWAS typically involves the integration of two independent datasets - an expression quantitative trait loci (eQTL) dataset and a genome-wide association study (GWAS) dataset.

A standard eQTL dataset consists of genetic variants (Z_j 's) and gene expression levels (X). Such datasets allow the discovery of eQTLs or genetic variants that affect gene expression levels. Notably, the Genotype-Tissue Expression (GTEx) project (GTEx Consortium, 2020), which comprises gene expression data across multiple tissues, has been instrumental in driving numerous genetic discoveries. Linear models are commonly used to assess the association between genetic variants and their gene expression levels:

$$\text{Genotype} - \text{GeneExpression (Model A)} : X = \alpha_{0,x} + \sum_{j=1}^p Z_j \beta_j + C^\top \alpha_x + \epsilon_x, \quad (2)$$

where $\alpha_{0,x}$ is the intercept; β_j 's and α_x are coefficients corresponding to Z_j 's and C , respectively; ϵ_x is the random error with mean zero. Furthermore, we denote X_Z as the component of gene expression level (X) that only depends on SNPs (Z), referred to as the genetically regulated gene expression levels. For example, in the aforementioned linear model, X_Z can be explicitly written as $X_Z := \sum_{j=1}^p Z_j \beta_j$.

As for GWAS data, direct access to raw GWAS data is often restricted, and most GWAS publications only report summary statistics, i.e., genetic variants and their associations

with specific phenotypes or traits, typically represented as estimated effect sizes and their standard errors, or p -values. GWAS typically assesses the marginal genetic association between the j th SNP and the trait Y assuming a classical linear model:

$$\text{Genotype} - \text{Trait (Model B)} : Y = \alpha_0 + Z_j \beta_{\text{GWAS},j} + C^\top \eta + e, \quad (3)$$

where α_0 is the intercept, $\beta_{\text{GWAS},j}$ and η are the coefficients regarding the j th SNP and covariates, and e is the random error.

While eQTL data encompasses expression levels of each gene, and GWAS assesses the SNP-phenotype associations, TWAS examines pair-wise associations between one gene and phenotype at a time. TWAS creates a foundation for direct gene-phenotype associations that are easier to interpret than SNP associations in GWAS and additionally may provide concrete targets for therapeutic development (Barbeira et al., 2018; Hu et al., 2019). With only GWAS summary statistics available, the main interest is to learn the association between Y and X_Z . Under the linear model setting eq (1)-(2), γ equivalently represents the association between Y and X and the association between Y and X_Z .

Two assumptions are commonly made in the existing TWAS literature to facilitate separating the genetic-contributed gene expression from the covariate (non-genetic)-contributed gene expression and deriving the test statistics in a GeneExpression-Trait model (Model C) through the information available from the GWAS model (Model B) and a Genotype-GeneExpression model (Model A).

Assumption 1. *The SNP set (Z_1, \dots, Z_p) is independent of the covariates C .*

This assumption is reasonable as most covariates are postnatal and related to environmental (non-genetic) factors. It also enables us to model genetic effects and covariate effects separately. Thus, we are able to test the association between the trait, and the genotype-contributed gene expression X_Z only.

Assumption 2. *The SNP set (Z_1, \dots, Z_p) only affects Y through X .*

This assumption implies that there are no other direct or indirect effects from Z on Y other than X_Z . This assumption is satisfied under most scenarios but could be violated, for example, because of *trans-eQTL*, i.e., eQTLs that act on distant genes, possibly outside of the 1Mb region or genes on other chromosomes. Identifying trans-eQTL is much more challenging due to a large number of SNP-gene pairs, and trans-eQTLs tend to have weaker effects than cis-eQTL (Pierce et al., 2014). Thus, most TWAS methods are focused on cis-eQTLs. This assumption also indicates that (Z_1, \dots, Z_p) is associated with, but not necessarily causal for X .

Based on Assumptions 1-2, existing TWAS methods train Model A (eq (2)) using eQTL data, and $H_0 : \gamma = 0$ is tested by replacing the unobserved X in Model C (eq (1)) by its conditional expectation on Z , $\mathbb{E}(X | Z)$. The test statistic for γ can be derived based on β_j in Model A (eq (2)) and the summary statistics $\beta_{\text{GWAS},j}$ in Model B (eq (3)) without requiring individual-level data in GWAS.

2.2 Proposed Statistical Model for SNP-gene-trait associations

As the main goal of TWAS is to test the association between the SNP-contributed gene expression levels (i.e., $X|Z$) and the trait Y , we propose to relax the linear association assumption in Model C (eq (1)) by a general additive model:

$$\text{New Model C : } Y = g_1(X_Z) + g_2(C) + \epsilon_y, \quad (4)$$

where $g_1(\cdot)$, and $g_2(\cdot)$ are unknown functions. The covariates effect in eq (2) and eq (1) are included in $g_2(C)$. The main goal of inference is $g_1(\cdot)$, which allows for a nonlinear association between Y and X_Z . When g_1 and g_2 are linear functions, eq (4) degenerates to the linear model in traditional TWAS (eq (1)). Note that the interaction effect of X and C

is not the main goal in TWAS, and estimating or testing the interaction effect is infeasible based on only GWAS summary statistics. More complex models $g(X_Z, C)$ could be explored in future research for cases where individual-level GWAS data are available. The proposed QTWAS model assumes Assumptions 1-2 as other TWAS approaches designed for GWAS summary statistics.

For ease of representation we denote $A_k = \{Q_{X_Z}(\tau_k), Q_{X_Z}(\tau_{k+1})\}$ as the region from the τ_k th quantile to the τ_{k+1} th quantile of the distribution of X_Z ; $\cup_k A_k$ covers the range of X_Z values. Though $g_1(\cdot)$ is unknown, it can be approximated by a piecewise linear function:

$$g_1(X_Z) \approx \sum_{k=1}^K \gamma_k X_Z I\{X_Z \in A_k\}, \quad (5)$$

where $I(\cdot)$ is an indicator function. Thus, we can approximately write model (1) as follows:

$$Y \approx \sum_{k=1}^K \gamma_k X_Z I\{X_Z \in A_k\} + g_2(C) + \epsilon. \quad (6)$$

Then, testing the gene-trait association through gene expression is equivalent to testing the null hypothesis:

$$H_0 : \gamma_k = 0 \text{ for } k = 1, \dots, K; \quad H_a : \text{at least one } \gamma_k \neq 0.$$

Based on eq (6), $\gamma_k = \arg \min_{\gamma} \mathbb{E}_Y (Y - \gamma_k X_Z)^2 I\{X_Z \in A_k\}$. Thus, the slope coefficient γ_k assesses the localized gene-trait association within a quantile sub-region of X_Z , which can be written as

$$\gamma_k = \frac{\text{cov}(X_Z, Y \mid X_Z \in A_k)}{\text{var}(X_Z \mid X_Z \in A_k)}, \text{ for } k = 1, \dots, K. \quad (7)$$

The above eq (7) implies that A_k cannot be too small; otherwise, the estimation of $\text{var}(X_Z \mid X_Z \in A_k)$ will be highly unstable. Meanwhile, A_k cannot be too large, as that would lead to a poor estimation of the unknown function $g_1(\cdot)$ according to eq (5). Our recommendation for choosing A_k based on empirical studies is discussed in Section 2.6.

In Section 2.3, we show that the coefficient γ_k can be estimated by leveraging a conditional quantile process model of the gene expression and GWAS summary statistics. The key idea is to decompose the covariance $cov(X_Z, Y \mid X_Z \in A_k)$ in eq (7) by the law of total variance:

$$\begin{aligned} cov(X_Z, Y \mid X_Z \in A_k) &= \mathbb{E}\{cov(X_Z, Y \mid Z, X_Z \in A_k)\} \\ &\quad + cov\{\mathbb{E}(X_Z \mid Z, X_Z \in A_k), \mathbb{E}(Y \mid Z, X_Z \in A_k)\}. \end{aligned} \quad (8)$$

As Assumption 2 implies the conditional independence $Y \perp\!\!\!\perp X_Z \mid Z$, the covariance is determined by the correlations between $\mathbb{E}(X_Z \mid Z, X_Z \in A_k)$ and $\mathbb{E}(Y \mid Z, X_Z \in A_k)$. In the following sections, we first train the quantile prediction model from the gene expression data (e.g., GTEx) to estimate the conditional quantile function of gene expression given a genotype profile and obtain $\mathbb{E}(X_Z \mid Z, X_Z \in A_k)$ (Section 2.3). Then, we construct test statistics by integrating GWAS summary statistics through $\mathbb{E}(Y \mid Z, X_Z \in A_k)$ with the estimated quantiles of gene expressions (Section 2.4).

2.3 Modeling the conditional distribution of $X_Z \mid Z$

Define $Q_X(\tau \mid Z, C)$ as the conditional quantile of gene expression X given genotypes Z and covariates C . We describe how to use quantile regression models (Koenker and Bassett, 1978) to estimate $\mathbb{E}(X_Z \mid Z, X_Z \in A_k)$ without prior knowledge of functions f_1 and f_2 .

We assume the following linear quantile model for $Q_X(\tau \mid Z, C)$:

$$Q_X(\tau \mid Z, C) = \alpha_0(\tau) + C^\top \alpha(\tau) + Z^\top \beta(\tau) \quad \text{for all } \tau \in (0, 1), \quad (9)$$

where $\alpha_0(\tau)$, $\alpha(\tau)$, and $\beta(\tau)$ are quantile-specific intercepts and slopes for covariates and genotypes, respectively. Denote the GTEx data with one specific tissue as $\{X_i, \mathbf{Z}_i, \mathbf{C}_i\}_{i=1}^n$ with sample size n , where $\mathbf{Z}_i = (Z_{i1}, \dots, Z_{ip})$ and $\mathbf{C}_i = (C_{i1}, \dots, C_{iq})$. For a fine grid of

$\tau \in (0, 1)$, we estimate $\beta(\tau)$ by solving

$$(\hat{\alpha}_{0,\tau}, \hat{\alpha}_\tau, \hat{\beta}_\tau) = \arg \min_{\alpha_{0,\tau}, \alpha_\tau, \beta_\tau} \sum_i^n \rho_\tau(X_i - \alpha_{0,\tau} - \mathbf{C}_i \alpha_\tau - \mathbf{Z}_i \beta_\tau),$$

where $\rho_\tau(u) = |u|\{(1 - \tau)I(u < 0) + \tau I(u > 0)\}$ is the quantile regression check function with $u \in \mathbb{R}$, and $I(\cdot)$ is an indicator function. Denote F_X as the CDF of X ; then the quantile function can be written as the inverse of the CDF: $Q_X(\tau) = F_X^{-1}(\tau)$. Furthermore, because the quantile function Q is an “almost sure left inverse” for the distribution function F (i.e., $Q(F(X)) = X$ almost surely), the distribution of the gene expression X can be obtained by $\alpha_0(U) + C^\top \alpha(U) + Z^\top \beta(U)$, where $U \sim \text{Unif}(0, 1)$. One can view the distribution of gene expression X as a convolution of a genotype-related random variable $Z^\top \beta(U)$ and another nongenotype-related random variable $\alpha_0(U) + C^\top \alpha(U)$. It follows that genotype-related gene expression X_Z has the same distribution as $Z^\top \beta(U)$. Thus,

$$\mathbb{E}(X_Z \mid Z, X_Z \in A_k) = \int_{\tau_k}^{\tau_{k+1}} Z^\top \beta(u) du = Z^\top \beta_{A_k},$$

where $\beta_{A_k} := \int_{\tau_k}^{\tau_{k+1}} \beta(u) du$. Accordingly, we have $\hat{\beta}_{A_k} = \int_{\tau_k}^{\tau_{k+1}} \hat{\beta}(\tau) d\tau$, in which τ_k and τ_{k+1} define the range of A_k .

2.4 Testing the quantile-stratified gene-trait association

Denote $\hat{\gamma}_k$ as the estimate of γ_k for region A_k , $se(\hat{\gamma}_k)$ as the standard error of $\hat{\gamma}_k$, and N_{GWAS} as the sample size for GWAS data. The z score for the gene-trait association for region A_k is $\mathcal{Z}_k = \hat{\gamma}_k / se(\hat{\gamma}_k)$. Given eq (7)–(8) and the conditional independence assumption $Y \perp\!\!\!\perp X_Z \mid Z$, we have that $\mathbb{E}\{cov(X_Z, Y \mid Z, X_Z \in A_k)\} = 0$, and $\mathbb{E}(Y \mid Z, X_Z \in A_k) = Z^\top \beta_{\text{GWAS}}$, where β_{GWAS} is the SNP-level effect size. With σ_j representing the standard deviation of

the j -th SNP, we have

$$\begin{aligned}
& cov\{\mathbb{E}(X_Z \mid Z, X_Z \in A_k), \mathbb{E}(Y \mid Z, X_Z \in A_k)\} \\
&= cov(Z^\top \beta_{A_k}, Z^\top \beta_{\text{GWAS}}) \\
&= \beta_{A_k}^\top var(Z) \beta_{\text{GWAS}},
\end{aligned}$$

such that

$$\hat{\gamma}_k = \frac{\hat{\beta}_{A_k}^\top}{\hat{\sigma}_{X_Z \in A_k}^2} var(Z) \hat{\beta}_{\text{GWAS}},$$

where $\hat{\sigma}_{X_Z \in A_k}^2$ is the variance of imputed gene expression in the region A_k , acting as an estimate of $\sigma_{X_Z \in A_k}^2 := var(X_Z \mid X_Z \in A_k)$, and $\hat{\beta}_{\text{GWAS}}$ is the SNP-level estimated effect size available from GWAS summary statistics. Regarding $se(\hat{\gamma}_k)$, we have

$$se(\hat{\gamma}_k) = \sqrt{\frac{var(\epsilon_y)}{N_{\text{GWAS}} var(X_Z \mid X_Z \in A_k)}} \approx \frac{\hat{\sigma}_Y}{\sqrt{N_{\text{GWAS}}} \hat{\sigma}_{X_Z \in A_k}},$$

where $\hat{\sigma}_Y$ is the estimated standard deviation of trait Y . We have $var(\epsilon_y) \approx \sigma_Y^2$ based on the empirical observation that only a very small proportion of the variability of the trait can be explained by any single gene (Hu et al., 2019; O'Connor et al., 2017). We then use the same argument for the SNP-level association statistics in GWAS data. For the j th SNP in the model, its z score can be denoted as

$$\tilde{z}_{\text{GWAS},j} = \frac{\hat{\beta}_{\text{GWAS},j}}{se(\hat{\beta}_{\text{GWAS},j})} \approx \frac{\sqrt{N_{\text{GWAS}}} \hat{\sigma}_j \hat{\beta}_{\text{GWAS},j}}{\hat{\sigma}_Y},$$

where $\hat{\sigma}_j$ is the estimated standard deviation of the j -th SNP. The matrix form of GWAS z score is

$$\tilde{\mathbf{z}}_{\text{GWAS}} \approx \frac{\sqrt{N_{\text{GWAS}}}}{\hat{\sigma}_Y} \text{diag}\{\hat{\sigma}_1, \dots, \hat{\sigma}_p\} \hat{\beta}_{\text{GWAS}}.$$

Of note, $\hat{\beta}_{\text{GWAS},j}$ is obtained from a marginal linear regression model (eq (3)). If a multivariate linear model (denoted as ‘‘MV’’) is fitted with p SNPs together, one would have

$\tilde{\mathbf{z}}_{\text{MV}} \approx \frac{\sqrt{N_{\text{GWAS}}}}{\hat{\sigma}_Y} \{var(Z)\}^{1/2} \hat{\beta}_{\text{GWAS}}$, and $\tilde{\mathbf{z}}_{\text{MV}} \approx N(0, I_p)$ under the null hypothesis (i.e.,

no SNP-trait association). Denote D_Z as the correlation matrix of the genotype matrix Z , which is also called the linkage-disequilibrium matrix in genetics. Given that $\text{var}(Z) = \text{diag}\{\sigma_1, \dots, \sigma_p\} D_Z \text{diag}\{\sigma_1, \dots, \sigma_p\}$, it follows that the z score obtained from GWAS $\tilde{\mathcal{Z}}_{\text{GWAS}} = D_Z^{1/2} \tilde{\mathcal{Z}}_{MV} \approx N(0, D_Z)$ under the null hypothesis.

Combining the derivations above, we have the gene-level quantile-stratified z score

$$\begin{aligned} \mathcal{Z}_k = \frac{\hat{\gamma}_k}{\text{se}(\hat{\gamma}_{A_k})} &\approx \frac{1}{\hat{\sigma}_{X_Z \in A_k}} \hat{\beta}_{A_k}^\top \{\text{var}(Z)\}^{1/2} \tilde{\mathcal{Z}}_{MV} \\ &= \frac{1}{\hat{\sigma}_{X_Z \in A_k}} \hat{\beta}_{A_k}^\top \text{diag}\{\hat{\sigma}_1, \dots, \hat{\sigma}_p\} \tilde{\mathcal{Z}}_{\text{GWAS}}. \end{aligned} \quad (10)$$

Similar to other TWAS approaches, e.g. Hu et al. (2019); Barbeira et al. (2018), the quantities obtained from the gene expression data, such as $\hat{\sigma}_{X_Z \in A_k}$, $\hat{\sigma}_j$'s, and $\hat{\beta}_{A_{X_Z}, k}$ are treated as fixed in the GWAS data. Hence, under $H_0 : \gamma_k = 0$ for $k = 1, \dots, K$, $\Delta^{-1/2} \mathcal{Z}_k \approx N(0, I)$, where $\Delta = \frac{1}{\hat{\sigma}_{X_Z \in A_k}^2} \hat{\beta}_{A_k}^\top \text{diag}\{\hat{\sigma}_1, \dots, \hat{\sigma}_p\} D_Z \text{diag}\{\hat{\sigma}_1, \dots, \hat{\sigma}_p\} \hat{\beta}_{A_k}$, and D_Z can be calculated from GTEx data or other external reference data. The p -value for testing $\gamma_k = 0$ in each region A_k can be computed as $p_k = 2\Phi(-|\mathcal{Z}_k|)$, where $\Phi(\cdot)$ is the normal CDF. Finally, we combine all p_k 's from K regions by the Cauchy combination method (Liu and Xie, 2020). Let p_1, \dots, p_K be K p -values. The Cauchy combination method shows that the test statistic $\sum_{k=1}^K \tan\{(0.5 - p_k)\pi\}/K$ follows a standard Cauchy distribution for arbitrary K regardless of the correlations among p -values, which provides an analytical form and avoids time-consuming numerical permutations. Other methods for p -value combination are possible, such as the minimum p -value, higher criticism, Fisher's method, and Berk-Jones (Dudoit et al., 2003; Fisher, 1992; Jin, 2006; Moscovich et al., 2016; Sun et al., 2019). We summarize the flowchart of QTWAS in Figure 2, and a discussion on selecting K is provided in Section 2.6.

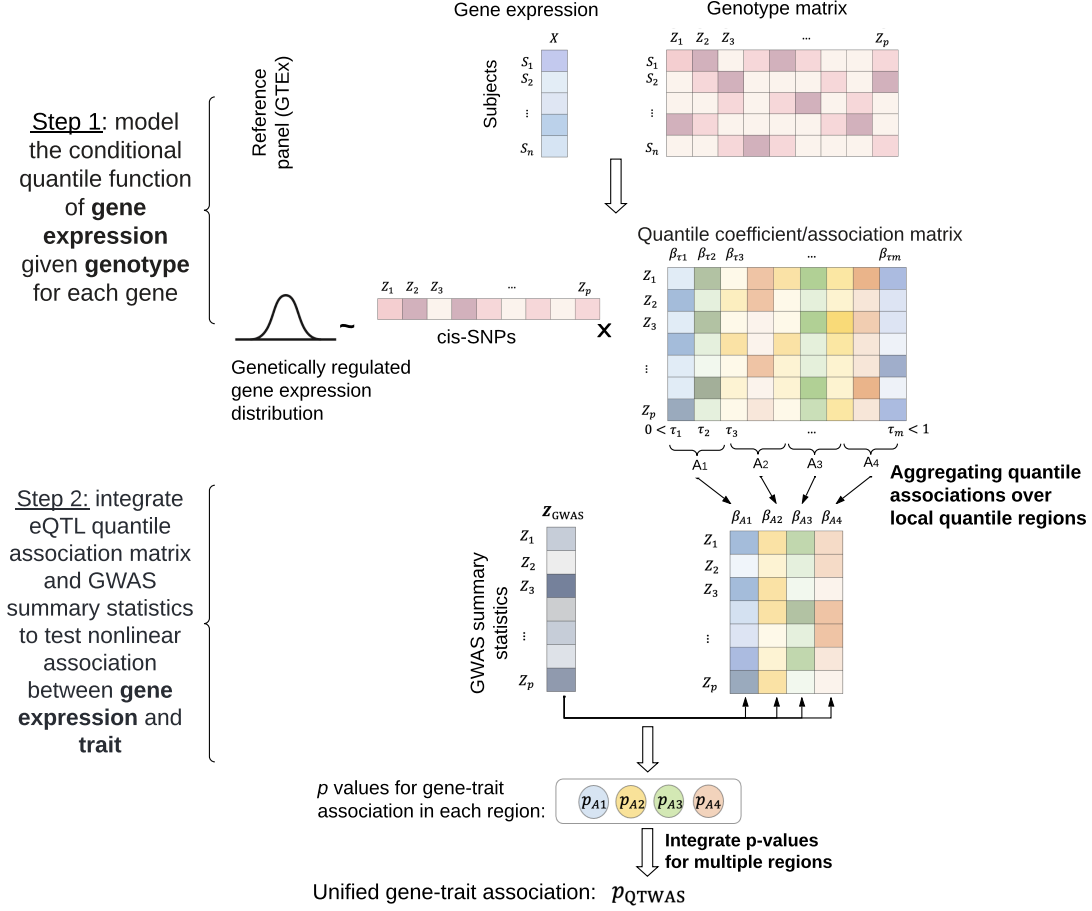


Figure 2: QTWAS flowchart with a specific region partition ($K = 4$).

2.5 From linear models to generalized linear models

Though the derivation of the QTWAS test statistics above assumes a linear GWAS model, that is, a continuous Y , we show that the derivation applies to generalized linear models with any link function. We denote the GWAS data as $\{Y_m, \mathbf{Z}_m, \mathbf{C}_m\}_{m=1}^{N_{\text{GWAS}}}$, with $\mathbf{Z}_m = (Z_{m1}, \dots, Z_{mp})$ and $\mathbf{C}_m = (C_{m1}, \dots, C_{mq})$. Assume there is an arbitrary link function $h(\cdot)$, such that $\mathbb{E}(Y_m \mid Z_{mj}, \mathbf{C}_m) = h(\alpha_0 + Z_{mj}\beta_{\text{GWAS},j} + \mathbf{C}_m\eta)$ and $\mathbb{E}(Y_m \mid X_{Z,m}, \mathbf{C}_m) = h(g_1(X_{Z,m}) + g_2(\mathbf{C}_m))$. Common link functions include $h(x) = \exp(x)/(1 + \exp(x))$ for logistic regression, $h(x) = x$ for linear regression, $h(x) = \exp(x)$ for loglinear models.

Though the GWAS summary statistics, including $\hat{\beta}_{\text{GWAS},j}$ and $se(\hat{\beta}_{\text{GWAS},j})$, could be estimated from generalized linear models, one can treat them as if they were estimated from linear regression with pseudo-response Y_i^* such that

$$\text{Model B : } Y_m^* = h^{-1}\{\mathbb{E}(Y_m \mid Z_{mj}, \mathbf{C}_m)\} + \epsilon_m^* = \alpha_0 + Z_{mj}\beta_{\text{GWAS},j} + \mathbf{C}_m\eta + \epsilon_m^*,$$

and

$$\text{Model C : } Y_m^* = h^{-1}\{\mathbb{E}(Y_m \mid X_{Z,m}, \mathbf{C}_m)\} + e_m^* = g_1(X_{Z,m}) + g_2(\mathbf{C}_m) + e_m^*,$$

where $\mathbb{E}(\epsilon_m^*) = \mathbb{E}(e_m^*) = 0$ and $var(\epsilon_m^*) \approx var(e_m^*) \approx \sigma_{Y^*}^2$. A reasonable estimation for $\sigma_{Y^*}^2$ is $\sqrt{N_{\text{GWAS}}}\hat{\sigma}_j se(\hat{\beta}_{\text{GWAS},j})$ based on the derivation of $se(\hat{\beta}_{\text{GWAS},j})$, where $\hat{\sigma}_j$ is the estimated standard deviation of the j -th SNP. Therefore, the GWAS summary statistics $\{\hat{\beta}_{\text{GWAS},j}, se(\hat{\beta}_{\text{GWAS},j})\}$, which is estimated based on $\{Y_m, Z_{mj}, \mathbf{C}_m\}_{m=1}^{N_{\text{GWAS}}}$ by generalized linear models, can be equivalently viewed as the GWAS summary statistics estimated from linear models with $\{Y_m^*, Z_{mj}, \mathbf{C}_m\}_{m=1}^{N_{\text{GWAS}}}$, and the derivation of the QTWAS statistics remains valid. Hence, one can use GWAS summary statistics in eq (10) regardless of the models they were generated from.

2.6 Model implementation and evaluation

Variant screening procedure. Based on empirical evidence, X_Z often depends on a sparse set of SNPs (Barbeira et al., 2018; Gamazon et al., 2015). Most existing TWAS approaches use penalized linear regression to select significant SNPs associated with the mean of X_Z (Barbeira et al., 2018; Gamazon et al., 2015; Hu et al., 2019), which may not be optimal at identifying more local (quantile-stratified) associations. We introduce a new variant screening procedure based on the quantile rank score test to identify important SNPs separately for each region A_k . The new screening procedure is more effective

at identifying heterogeneous distributional associations and non-gaussian errors. We outline the detailed algorithm below and provide a flowchart of the screening procedure in the Appendix (Section 1). Specifically, we aggregate multiple quantile rank score tests (Gutenbrunner et al., 1993) at selected quantile levels within $A_{X,k}$ to select region-specific SNPs. For each variant located within $\pm 1\text{Mb}$ of a gene’s transcription start site (TSS), we first perform quantile rank score test (Gutenbrunner and Jurecková, 1992; Song et al., 2017) on several quantile levels selected from the target quantile intervals $A_{X,k}$ ’s and then combine multiple p -values using the Cauchy combination method (Liu and Xie, 2020). We select significant variants while controlling the false discovery rate at the 5% level using the method of Benjamini and Hochberg (1995). Among the selected SNPs, we further filtered out highly correlated SNPs via hierarchical clustering (more details are described in Appendix Section 1) and used the final set of SNPs as the Z matrix used in model (9). Note that the variant screening step is a data pre-processing procedure for training the Genotype-GeneExpression model by GTEx data, which is independent of the subsequent steps for constructing test statistics. Thus, it does not affect the multiple testing burden at the gene-level QTWAS p -values.

Implementation details in the GTEx data. We trained the gene expression prediction model for 49 tissues from the GTEx project (v8), as described below. Gene expression levels were normalized and adjusted for covariates and confounders, including sex, sequencing platform, and the top five principal components of genotype data, as well as the top 15 probabilistic estimation of expression residuals (PEER) factors (Hu et al., 2019; Stegle et al., 2010). We considered protein-coding genes, removed ambiguously stranded SNPs, and only considered ref/alt pairs A/T, C/G, T/A, and G/C. SNPs with minor allele frequency less than 0.01 were excluded from the analyses. For each gene, we used SNPs

between 1Mb upstream and downstream of the transcription start site. The LD matrix D_Z is estimated from the genotype data in the GTEx data.

Selection of K . The length of A_k and the number of regions (K) can be set depending on applications. Though the piecewise linear approximation eq (5) assumes $\cup_{k=1}^K A_k = (0, 1)$ for estimation, it can be relaxed in the context of hypothesis testing. To test the overall associations between X_Z and Y , integrating $\beta(\tau)$'s over a larger region A_k is especially helpful in detecting weak genetic associations. Based on our empirical experience, $K = 3$ or 4 would be sufficient to detect homogeneous associations, such as location shift, and a relatively larger K (e.g., $K = 9$) facilitates detecting local associations, whereas a very large K is not recommended because of the risk of power loss. As the underlying association patterns are unknown in real applications, one can further consider using partially overlapped regions and multiple choices of K to improve the power. In practice, we use the Cauchy combination method to combine results from $K \in \{3, 4, 5, 9\}$ with slightly overlapped regions to obtain robust and powerful results (see the region segments in Appendix Section 1). This approach is data-driven, insensitive to the underlying association patterns, and avoids selecting K as a tuning parameter. Furthermore, for a specified K , we recommend considering the partition such that $\cup_{k=1}^K A_k$ covers the 5% percentile to the 95% percentile of the value of X_Z . We do not recommend considering $\tau < 0.05$ and $\tau > 0.95$, as coefficients of extreme quantiles are more challenging to estimate. Excluding the extreme regions $\tau \in (0, 0.05)$ and $\tau \in (0.95, 1)$ may lead to loss of power if the local association only exists at the extreme tails. Investigators can set the regions based on applications; the specific regions we used are provided in Appendix Section 1 as an illustration.

3 Simulation studies

3.1 Simulation settings

The simulation studies are based on the data in the whole blood tissue from GTEx v8 ($n = 670$). We generate gene expression based on the genotype data on 670 individuals from GTEx (see details below on the genotype-gene expression models). Then, we resample $n = 1000$ subjects and generate their trait values based on their genotypes. For each gene, Z includes all SNPs within ± 1 Mb from its TSS. Gene expression X is normalized before analysis as common practice in genetic association tests. The set of covariates C includes the top five principal components, top 15 PEER factors, platform, and sex. Similar to Hu et al. (2019), we randomly select 500 genes and generate the gene expression data and traits independently for each gene, as described below.

Null model. To evaluate Type I error, we generate the gene expression X from the model: $X = Z^\top \beta + C^\top \alpha_x + \epsilon_x$, in which β is estimated based on true GTEx data via the elastic net with the tuning parameter set as 0.5. The trait Y is generated by $Y = C^\top \eta + e$. Both error terms e and ϵ_x follow a standard normal distribution; α_x and η are vectors with each element randomly drawn from $\text{Unif}(0, 1)$. This null model preserves the associations between gene expression and SNPs from GTEx data but assumes no gene-trait association. A similar setting has been simulated in Hu et al. (2019).

Alternative models. For power analyses, we consider three different Genotype-GeneExpression models, and we assume a simple linear Genotype-Trait model to mimic the setting of GWAS summary statistics from linear models.

Genotype-GeneExpression models. We consider the following three models:

- (a) Location shift: $X = Z^\top \beta + C^\top \alpha_x + \epsilon_x$;
- (b) Location-scale: $X = Z^\top \beta + C^\top \alpha_x + (1 + 0.5G^\top \beta)\epsilon_x$;
- (c) Local signal: $Q_X(\tau > 0.7 \mid Z, C) = 5 \frac{\tau - 0.7}{1 - 0.7} Z^\top \beta + C^\top \alpha_x + F_{\epsilon_x}^{-1}(\tau)$.

In the location shift model (a), the genetic variants Z only affect the mean of X , while in the location-scale model (b), the genetic variants Z affect both the mean and variance of X . In the local signal model (c), the variants Z only affect part of the distribution of X (i.e., Z only affects the upper quantile (> 0.7 th quantile) of X). In each of the three scenarios, we consider two error distributions for ϵ_x : standard normal and Cauchy distributions, where the Cauchy distribution has been commonly considered as a challenging case of heavy-tailed distributions in genetic association studies (Song et al., 2017; Wang et al., 2022). Under models (b) and (c), when the quantile specific coefficients are different across quantiles, the Genotype-GeneExpression association is heterogeneous, and the transcriptome-wide association is nonlinear (Appendix Section 2.1).

Genotype-Trait model. We consider a simple linear model $Y = Z^\top \beta_{\text{GWAS}} + C^\top \eta + e$, where e follows a standard normal distribution.

To illustrate the performance in different scenarios, we randomly select 1% of SNPs from the 2Mb region around TSS to be causal (i.e., with non-zero effect sizes β and β_{GWAS}). We set $\beta_{\text{GWAS}} = \mathbf{1}_p$ and $\beta = 2 \cdot \mathbf{1}_p$ for local signal model, $\beta_{\text{GWAS}} = 0.2 \cdot \mathbf{1}_p$ and $\beta = 0.4 \cdot \mathbf{1}_p$ for location-scale model, and $\beta_{\text{GWAS}} = 0.1 \cdot \mathbf{1}_p$ and $\beta = 0.2 \cdot \mathbf{1}_p$ for location shift model, where $\mathbf{1}_p$ represents a column vector with all elements being 1. α_x and η are vectors with each element randomly drawn from $\text{Unif}(0, 1)$.

For power analyses, we repeat the data generation procedure two times per gene and report the statistical power based on 1,000 replicates at the significance threshold $\alpha = 2.5e-6$ (corresponding to the usual Bonferroni threshold when testing 20,000 protein-coding genes).

For type I error analysis, we repeat the procedure for each gene 20,000 times and report the results based on 10^7 replicates at different significance thresholds ranging from 0.05 to $2.5e - 6$. In addition, we compare the proposed framework with our own implementation of S-PrediXcan (note that we have re-implemented S-PrediXcan as it needs to be trained based on simulated data, and we denote it as “S-PrediXcan*”). For our method, we report results based on a single region partition ($K = 3/4/5/9$) and the unified results combining all partitions. The detailed partitions are described in Appendix Section 1. For one gene, we randomly generate $p \sim \text{Unif}(0, 1)$ if the elastic net model in S-PrediXcan* does not select any variables, or if none of the four regions A_1 - A_4 in QTWAS has valid p -value (e.g., no variant is selected).

3.2 Simulation results

Type I error analysis. The type I error for QTWAS, either with a single choice of K or a unified result based on four choices of K , is controlled at all significance levels (Table 1).

Power analysis. QTWAS, combining different quantile intervals, has improved power in most scenarios compared to S-PrediXcan* (Table 2). When the error is Gaussian, both methods have comparable power for the location shift and location-scale models. However, QTWAS has substantially improved power over S-PrediXcan* when the association is local and only at upper quantiles. When the error follows the Cauchy distribution, QTWAS performs well compared to S-PrediXcan. Additionally, we observe that QTWAS is not very sensitive to the choice of K , and the unified approach performs best.

We further illustrate the power improvement of QTWAS using the partition $K = 4$ as an example. We provide the figure of region-specific power of the QTWAS test statistics

α	S-PrediXcan*	<u>QTWAS</u>				
		Unified	$K = 3$	$K = 4$	$K = 5$	$K = 9$
0.05	5.024E-02	5.154E-02	4.993E-02	4.910E-02	4.924E-02	4.937E-02
1e-2	1.075E-02	9.784E-03	9.908E-03	1.017E-02	9.841E-03	9.843E-03
1e-3	1.248E-03	6.536E-04	9.267E-04	8.847E-04	1.004E-03	8.584E-04
1e-4	9.770E-05	3.900E-05	2.380E-05	6.140E-05	6.490E-05	5.910E-05
1e-5	4.600E-06	1.800E-06	1.700E-06	1.200E-06	1.300E-06	1.500E-06
2.5e-6	1.400E-06	1.200E-06	2.000E-07	3.000E-07	3.000E-07	1.200E-06

Table 1: Type I error results for S-PrediXcan* and QTWAS ($n_{\text{GTEx}} = 670$), as well as for quantile region stratified QTWAS based on 10^7 replicates. “Unified” combines the p -value of $K = 3/4/5/9$ via the Cauchy combination method.

<u>Normal Error</u>	S-PrediXcan*	<u>QTWAS</u>				
		Unified	$K = 3$	$K = 4$	$K = 5$	$K = 9$
Model						
location shift	0.999	0.996	0.995	0.995	0.994	0.995
location-scale	0.901	0.905	0.864	0.864	0.871	0.896
local signal	0.132	0.440	0.317	0.324	0.369	0.407

<u>Cauchy Error</u>	S-PrediXcan*	<u>QTWAS</u>				
		Unified	$K = 3$	$K = 4$	$K = 5$	$K = 9$
Model						
location shift	0.878	0.944	0.913	0.913	0.927	0.938
location-scale	0.392	0.611	0.500	0.534	0.541	0.603
local signal	0.115	0.372	0.263	0.269	0.298	0.331

Table 2: Power of S-PrediXcan* and QTWAS in location shift, location-scale, and local signal models with normal and Cauchy errors, respectively. The significance threshold is $\alpha = 2.5e - 6$. “Unified” combines the p -values of $K = 3/4/5/9$ via the Cauchy combination method.

under three models in Appendix Section 2.2. The power of QTWAS in each region reveals the true underlying signal. For example, the location shift model with normal errors has equally high power in each region, and the location-scale model with normal errors shows increasing power from lower quantile to upper quantile, corresponding to the assumptions of our model. For local signal models, we observed a dominant power boost for QTWAS, owing to the power of QTWAS test statistics in the upper quantile region (A_4), corresponding to the true signals being simulated at upper quantiles (i.e., $\tau > 0.7$). Therefore, the region-specific quantile test statistic can reveal more complex and detailed association patterns.

Under alternative models, we assess the robustness of the QTWAS approach. That is, we report how sensitive the QTWAS is to the choice of K . Among the significant results of QTWAS in Table 2, we report the proportion identified by at least two partitions with the significance threshold $2.5e - 6$ (see Appendix Section 2.2). We observe that most of the QTWAS discoveries are identified by at least two partitions for all models, with the proportion slightly decreasing for the models with a higher level of heterogeneity. Overall, these results suggest that QTWAS results are robust.

3.3 Model evaluation

Imputation accuracy. To evaluate the accuracy of the gene expression imputation model (9), we consider the goodness of fit criterion $R^Q(\tau) = 1 - \hat{V}(\tau)/\tilde{V}(\tau)$ (Koenker and Machado, 1999), a measurement of explained deviance by the quantile model associated to genetic effects at a fixed quantile level, where $\hat{V}(\tau) = \min \sum_i^n \rho_\tau(X_i - C_i^\top \alpha_\tau - Z_i^\top \beta_\tau - \alpha_{0,\tau})$ and $\tilde{V}(\tau) = \min \sum_i^n \rho_\tau(X_i - C_i^\top \alpha_\tau - \alpha_{0,\tau})$ are optimized quantile loss under the null and alternative models, respectively. It is a natural analog to R^2 in linear models. We use $K = 4$ as an example and consider the largest $R^Q(\tau)$ over the four intervals as the ex-

plained deviance by QTWAS, which coincides with the fact that the Cauchy combination is practically driven by the most significant p -value combined. To compare the imputation accuracy for QTWAS and S-PrediXcan*, we plotted R^Q against R^2 (Figure 3). Except for the location shift model with normal error, QTWAS generally explained more deviance than S-PrediXcan*. Specifically, in the location-scale and local signal models, S-PrediXcan* explains a low proportion of the total deviance, indicating a relatively poor goodness of fit compared to quantile models.

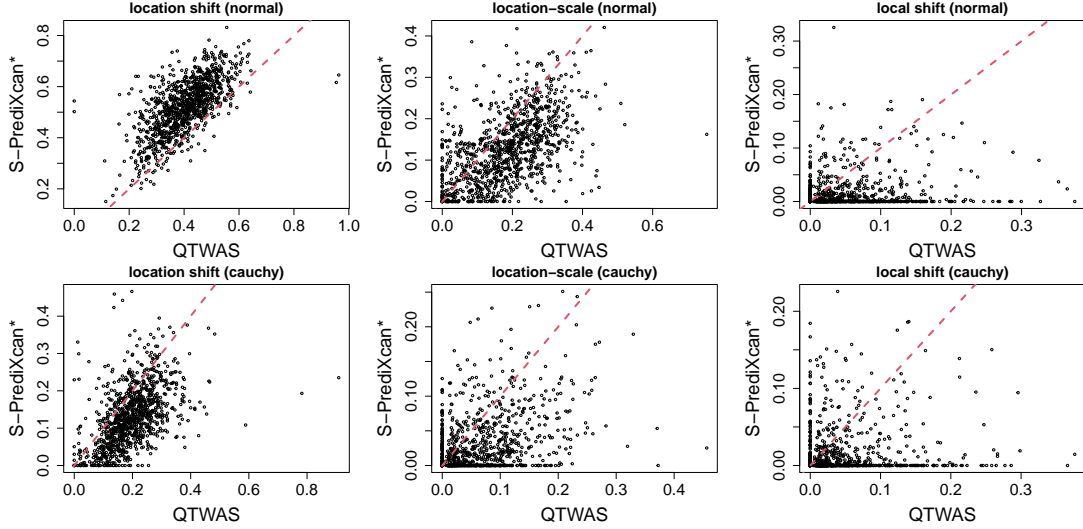


Figure 3: Model explained deviance for QTWAS and S-PrediXcan*. We consider the location shift, location-scale, and local signal models with normal errors and Cauchy errors.

Evaluation of variant screening procedure. To evaluate the quantile variant screening, we measure the canonical correlation between selected sets and the causal set in the three alternative models with normal or Cauchy errors. For ease of presentation, we again consider $K = 4$ as an example and use “QTWAS $_{A_k}$ ” to denote the results for region $k = 1, 2, 3, 4$. The proportion of replicates with a correlation greater than 0.95 is reported in Table 3 based on 1,000 replicates. For the location shift model, both QTWAS and S-PrediXcan* select SNP sets highly correlated with the true causal set. In the location-scale

model, the proportion of replicates selecting highly correlated SNPs is increasing with the quantile levels and is comparable to S-PrediXcan* for interval A_4 , consistent with the power results. In the local shift model, QTWAS selected a set of SNPs with high correlation with the true causal set in the upper quantile interval A_4 more often than S-PrediXcan*, as expected. The ability of QTWAS to select variants that are more correlated to the underlying causal variants in heterogeneous cases is likely due to the specific association-oriented screening procedure we use here.

Model	QTWAS _{A1}	QTWAS _{A2}	QTWAS _{A3}	QTWAS _{A4}	S-PrediXcan*
location shift	97.9%	99.1%	99.1%	99.0%	99.8%
location-scale	31.3%	54.2%	70.4%	83.7%	85.4%
local shift	4.5%	0.5%	0.5%	39.1%	15.4%

Table 3: The proportion of replicates (out of 1,000) with canonical correlation values between the selected variable set and the true causal set greater than 0.95.

3.4 Additional simulations

The previously presented local signal model is in favor of quantile regression, as the association only appears at upper quantiles. In the Appendix (Section 2.4), we consider two more models: $Q_X(\tau | Z, C) = Z^\top \beta(\tau) + C^\top \alpha_x + F_{\epsilon_x}^{-1}(\tau)$ with $\beta(\tau) = \sqrt{\tau}$ and $\beta(\tau) = \sin(2\pi\tau)$, respectively. Different from the previous local model, in which $\beta(\tau) \neq 0$ only for $\tau \in (0.7, 1)$, $\beta(\tau)$ here changes smoothly for $\tau \in (0, 1)$. For these two heterogeneous models, QTWAS also outperformed S-PrediXcan*. Specifically, QTWAS is powerful for the model with $\beta(\tau) = \sin(2\pi\tau)$ while S-PrediXcan* has almost no power because there is no association when $\tau = 0.5$. We further consider the location model with unobserved gene-environment interaction for the Genotype-GeneExpression model (Appendix Section 2.3). Results sug-

gest that when there exists gene-environment interaction, but the environmental factor is unobserved, QTWAS is equivalently powerful or more powerful than S-PrediXcan in detecting gene-trait associations.

We also compare the performance of S-PrediXcan and QTWAS to sMiST (Dong et al., 2020), a method based on mixed effect models. Though sMiST can also be performed based on summary statistics, the goal of sMiST is to test not only the total effect from imputed gene expression (e.g., similar to TWAS) but also the direct effect of genetic variants, which violates Assumption 2 in TWAS. Thus, the two threads of methods are not equivalent or directly comparable. Nevertheless, because of allowing a direct effect from SNPs to the trait, sMiST is more powerful than S-PrediXcan in the local model but still less powerful than QTWAS (see Appendix Section 2.5).

4 Application to LDL cholesterol

We apply S-PrediXcan and QTWAS to the publicly available GWAS summary statistics from UK Biobank (UKBB) from Pan-UKB team (2020). Specifically, we use the trait “LDL direct, adjusted by medication” (denoted as “LDL”, $N_{\text{GWAS}} = 398,414$) for illustration; we use whole-blood tissue from GTEx because of its large sample size relative to other tissues ($n = 670$). We consider different quantile partitions with $K \in \{3, 4, 5, 9\}$ and use the Cauchy combination to combine all p -values. For a more robust and convincing QTWAS result, among all genes identified by QTWAS, we only report genes that can be identified by at least two partitions. We focus on protein-coding genes and further restrict to the set of 6,560 genes with valid pre-trained S-PrediXcan models available from the PredictDB website (PredictDB Team, 2021). We provide a detailed analysis of the identified gene-trait associations, including both internal and external validations. For the internal validation,

we report the significant genes containing significant SNPs from UKBB summary statistics within the ± 1 Mb region from its TSS, and which are also reported eQTLs in GTEx. For the external validation, we use GWAS summary statistics from an independent LDL GWAS and report the number of genes that can be replicated by QTWAS and S-PrediXcan in this new dataset. To further understand the unique associations only identified by QTWAS, we present empirical results from both the Genotype-GeneExpression model in GTEx and the Genotype-Trait model in GWAS. We visualize the nonlinear association between genotype and gene expression in GTEx data, and we report the GWAS significant loci enriched in QTWAS-identified genes. We also applied the two methods to other continuous traits from UKBB and ten binary traits and summarized the results.

4.1 Results

The detailed comparison for QTWAS and S-PrediXcan at different significance levels (i.e., $2.5e - 6$, $1e - 10$, $1e - 15$, and $1e - 20$) is presented in Figure 4 (a). At all four significance levels, QTWAS consistently identified more associations. To validate those genes uniquely discovered by QTWAS, we take a further examination of the genes identified by both methods and only by QTWAS. For ease of presentation, we denote the group of genes only identified by QTWAS (or S-PrediXcan) as “QTWAS_only” (or “S-PrediXcan_only”) and the group of genes identified by both methods as “Both” in the rest of this section.

For internal validation, we first explore whether the “QTWAS_only” genes can also be identified by S-PrediXcan but at a lower significance level (e.g., a larger p -value). Figure 4 (b) shows that the overlapped proportion of “QTWAS_only” genes and the genes identified by S-PrediXcan at a lower significance level (i.e., $1e - 4$) is increasing with the increase of significance level from $2.5e - 6$ to $1e - 20$. This consistent trend shows that the genes only

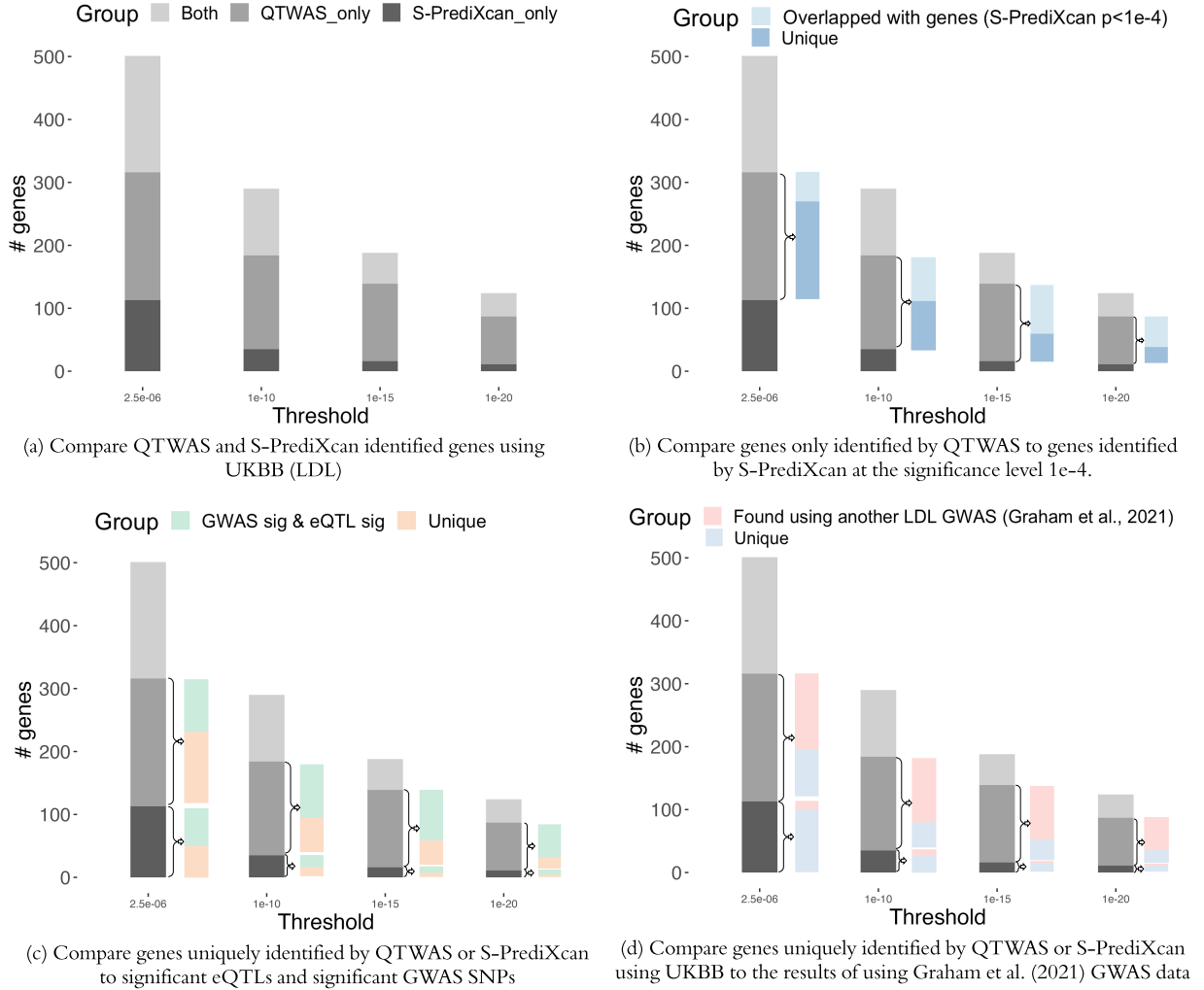


Figure 4: Validation results on genes identified by QTWAS and S-PrediXcan at different significant levels ($\alpha = 2.5e - 6, 1e - 10, 1e - 15$, and $1e - 20$).

identified by QTWAS at a specific significance level can be identified by S-PrediXcan at a lower significance level, suggesting that QTWAS is more powerful and S-PrediXcan may eventually be able to identify them with larger sample sizes. Next, for the “QTWAS_only” and “S-PrediXcan_only” genes, we also report the number of genes containing genome-wide significant SNPs ($p < 5e - 8$), which are also eQTLs for the same gene (from the GTEx portal website), within the $\pm 1\text{Mb}$ region from its TSS. With increased stringency of the significance level, we observed that the overlapped proportion for “QTWAS_only”

and “S-PrediXcan_only” genes is increasing, especially for “QTWAS_only” (Figure 4 (c)).

For the external validation, we explore the replicability of “QTWAS_only” and “S-PrediXcan_only” genes, either by QTWAS or S-PrediXcan, in independent GWAS data. Specifically, we use the GWAS summary statistics from Graham et al. (2021) because it contains a large number of European individuals, similar to the UKBB. The study of Graham et al. (2021) is a genome-wide genetic association meta-analysis of lipid levels with multi-ancestry, including 1.65 million individuals from 201 studies. Among all individuals, the major genetic ancestry group is European (79.8%). We compare the previous results based on UKBB with the genes identified in this GWAS by QTWAS and S-PrediXcan at the significance level $2.5e-6$. From Figure 4 (d), we observe that more than half of uniquely identified genes in UKBB by QTWAS can also be discovered using the GWAS summary statistics from Graham et al. (2021), and the reproducible proportion is increasing with increasing stringency of significance level. In contrast, most “S-PrediXcan_only” genes are not discovered using the summary statistics from Graham et al. (2021). The results suggest that QTWAS is indeed more powerful and “QTWAS_only” genes are more heterogeneous genes that are nonetheless replicated in independent studies.

4.2 Post-hoc analysis in GTEx and GWAS data

As the two-step TWAS framework combines both eQTL and GWAS information from two datasets, the genes only identified by QTWAS but not S-PrediXcan are highly likely to be detected due to nonlinear associations. For the highly significant genes ($p < 1e-20$) in “QTWAS_only” genes, we conjecture that the nonlinear association in the GTEx data (“GeneExpression model”) could be a major contributing factor. We present two genes, *LDLR* and *GSTM2*, as examples, which are highly significant with QTWAS but missed by

S-PrediXcan. *LDLR* is well-known to be associated with LDL (Goldstein and Brown, 2009), and *GSTM2* is reported to be associated with detoxification and metabolism (Wang et al., 2016). We define the burden score for the i th individual as $S_i = \sum_{j=1}^p \text{sign}(\hat{\beta}_{A_{X_Z,k,j}})X_{ij}$, where $\hat{\beta}_{A_{X_Z,k,j}}$ is estimated from the QTWAS model described in Section 2 for a specific region A_k . For both genes, we consider $\hat{\beta}_{A_{X_Z,k,j}}$ in the most significant region (i.e., smallest p -value among A_k 's): $\tau \in (0.55, 0.85)$ for *LDLR* and $\tau \in (0.3, 0.45)$ for *GSTM2*. After excluding the effect of the covariates, we plot the observed gene expression and burden score using the fitted curves by B-spline with a 95% bootstrap confidence interval. We observe clear nonlinear associations between the Burden Score and gene expression for both genes (Figure 5).

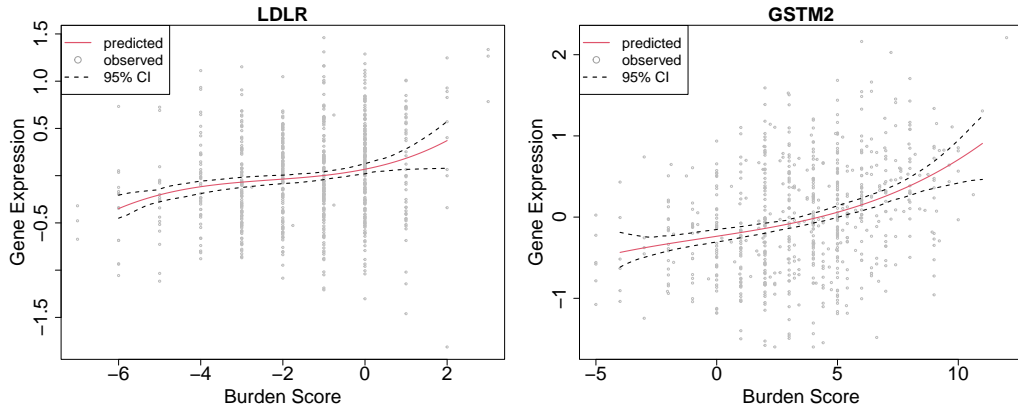


Figure 5: Nonlinear Genotype-GeneExpression association for *LDLR* (QTWAS p -value: 0 (the smallest Z score among all partitions < -55); S-PrediXcan p -value: 0.0628) and *GSTM2* (QTWAS p -value: $1.52e - 31$; S-PrediXcan p -value: 0.0028).

4.3 Additional results on 100 continuous traits and 10 binary traits

To compare the performance of the TWAS framework based on quantile regression, we further apply QTWAS and S-PrediXcan to 100 continuous traits that are closely related to whole blood tissue, such as lipid traits and blood cell counts, from UKBB. In particular, we consider the European population, for which the sample sizes are over 400,000 for more than 90% of these 100 traits. We also apply QTWAS and S-PrediXcan to summary statistics from ten GWAS studies on brain disorders with binary traits, including five neuropsychiatric traits: schizophrenia (SCZ, (Pardiñas et al., 2018)), attention-deficit/hyperactivity disorder (ADHD, (Demontis et al., 2019)), bipolar disorder (BD, (Stahl et al., 2019)), autism spectrum disorder (ASD, (Grove et al., 2019)) and major depressive disorder (MDD, (Howard et al., 2019)); and four neurodegenerative traits: Alzheimer’s disease (AD_Kunkle, (Kunkle et al., 2019); AD_Jansen, (Jansen et al., 2019)), Parkinson’s disease (PD, (Nalls et al., 2019)), multiple sclerosis (MS, (Andlauer et al., 2016)) and amyotrophic lateral sclerosis (ALS, (Van Rheenen et al., 2016)). Sample information for those studies is summarized in Appendix Section 3.1. Similarly, the reported QTWAS significant genes are identified by at least two partitions. For all 100 continuous traits and 10 binary traits, we observe that QTWAS consistently identified more genes than S-PrediXcan (see Figure 6). A complete list of the number of identified genes per trait is provided in Appendix Section 3.2.

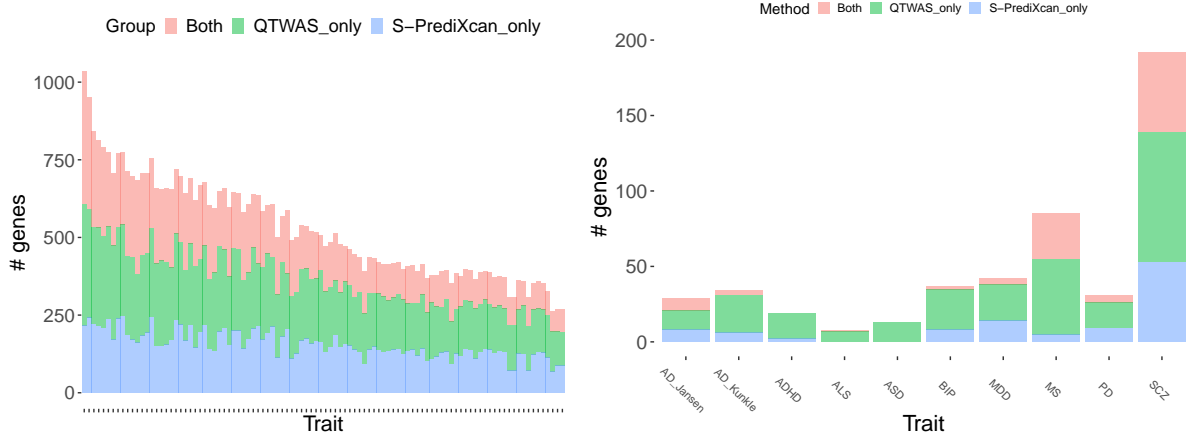


Figure 6: Results on QTWAS and S-PrediXcan identified genes on 100 UKBB traits related to whole blood tissue (**Left**) and 10 brain disorders (**Right**). "QTWAS_only" represents the number of genes only identified by QTWAS; "S-PrediXcan_only" represents the number of genes only identified by S-PrediXcan; "Both" represents the number of genes identified by both methods. The significance threshold is $2.5e-6$.

5 Discussion

We have proposed a novel quantile-based TWAS approach to effectively leverage expression reference panels and GWAS summary statistics to discover nonlinear gene-trait associations. Quantile regression tools have been previously proposed in the context of genetic association studies (Wang et al., 2022; Song et al., 2017; Wang et al., 2023). However, this is the first quantile-process-based method in TWAS. A key reason for its appeal is the promise of prioritizing candidate causal genes whose expression levels mediate the phenotypic effects in a dynamic and non-linear manner. As shown in both simulations and applications, such quantile models are able to identify more associations and provide more insights into how gene expression levels regulate phenotypes. In addition, the interval-based variant screening through quantile rank test leads to a more accurate and detailed imputation of gene expression in specific quantile intervals.

Compared to the mean-based approach S-PrediXcan, QTWAS showed more robust and promising discoveries across different traits. In general, a large number of genes discovered by S-PrediXcan are also identified by QTWAS. In addition, QTWAS is more powerful, discovering more new loci. Through validation analyses, we show that the novel genes identified by QTWAS are likely to be functional and relevant to the trait under study. Note that, like other TWAS approaches, QTWAS inevitably identifies multiple hit genes per locus due to LD confounding and co-regulation (Wainberg et al., 2019), and hence fine-mapping such loci can further prioritize relevant genes at each locus (Ma et al., 2023, 2021).

Several emerging topics in TWAS are left for future work. For the current single-tissue QTWAS framework, we recommend a larger sample size of eQTL data, such as the whole blood tissue we considered from GTEx, which leads to more robust and trustworthy results. For future research, it is desirable to develop approaches that combine data on multiple tissues to increase the total sample size of eQTL studies for the estimation of the conditional distribution of gene expression. Such approaches have been developed before, e.g., UTMOST (Hu et al., 2019), and have been shown to effectively increase imputation accuracy and power. Multi-tissue quantile modeling may allow investigations of more comprehensive nonlinear associations across tissues. Furthermore, the current QTWAS framework can be better developed when individual GWAS data are available, which would allow nonparametric approaches to estimate higher-resolution nonlinear gene-trait associations and multiplicative errors instead of additive errors, depending on the original transformation applied to the trait.

SUPPLEMENTARY MATERIAL

Appendix: The appendix includes a detailed variant screening procedure, additional sim-

ulation results, visualizing nonlinear gene-level association under alternative models, and more figures and tables for data analysis.

Data availability and web resources: We use data from existing studies from GTEx (v8, <https://gtexportal.org/home/>) and summary level GWAS results on the 10 neuropsychiatric and neurodegenerative traits (Pardiñas et al., 2018; Demontis et al., 2019; Stahl et al., 2019; Grove et al., 2019; Howard et al., 2019; Kunkle et al., 2019; Jansen et al., 2019; Nalls et al., 2019; Andlauer et al., 2016; Van Rheenen et al., 2016). The summary level GWAS results on the 100 UKBB traits, including the LDL, can be downloaded from the website: <https://pan.ukbb.broadinstitute.org/>. In data analyses, we use pre-trained models for S-PrediXcan. The models are available on the PredictDB website (PredictDB Team, 2021) (<https://predictdb.org/post/2021/07/21/gtex-v8-models-on-eqtl-and-sqtl/>).

Code availability: We have implemented the proposed QTWAS framework in R, and it is available on Dropbox (https://www.dropbox.com/sh/h3w11e9155qarz3/AAAM85NogUe1_QNZUDruD55_a?dl=0).

References

- Andlauer, T. F., D. Buck, G. Antony, A. Bayas, L. Bechmann, A. Berthele, A. Chan, C. Gasperi, R. Gold, C. Graetz, et al. (2016). Novel multiple sclerosis susceptibility loci implicated in epigenetic regulation. *Science advances* 2(6), e1501678.
- Barbeira, A. N., S. P. Dickinson, R. Bonazzola, J. Zheng, H. E. Wheeler, J. M. Torres, E. S. Torstenson, K. P. Shah, T. Garcia, T. L. Edwards, et al. (2018). Exploring the

- phenotypic consequences of tissue specific gene expression variation inferred from gwas summary statistics. *Nature communications* 9(1), 1825.
- Benjamini, Y. and Y. Hochberg (1995). Controlling the false discovery rate: a practical and powerful approach to multiple testing. *Journal of the Royal Statistical Society. Series B (Methodological)*, 289–300.
- Budinska, E., V. Popovici, S. Tejpar, G. D’Ario, N. Lapique, K. O. Sikora, A. F. Di Narzo, P. Yan, J. G. Hodgson, S. Weinrich, et al. (2013). Gene expression patterns unveil a new level of molecular heterogeneity in colorectal cancer. *The Journal of pathology* 231(1), 63–76.
- Demontis, D., R. K. Walters, J. Martin, M. Mattheisen, T. D. Als, E. Agerbo, G. Baldurs-son, R. Belliveau, J. Bybjerg-Grauholm, M. Bækvad-Hansen, et al. (2019). Discovery of the first genome-wide significant risk loci for attention deficit/hyperactivity disorder. *Nature genetics* 51(1), 63–75.
- Dong, X., Y.-R. Su, R. Barfield, S. A. Bien, Q. He, T. A. Harrison, J. R. Huyghe, T. O. Keku, N. M. Lindor, C. Schafmayer, et al. (2020). A general framework for functionally informed set-based analysis: application to a large-scale colorectal cancer study. *PLoS genetics* 16(8), e1008947.
- Dudoit, S., J. P. Shaffer, J. C. Boldrick, et al. (2003). Multiple hypothesis testing in microarray experiments. *Statistical Science* 18(1), 71–103.
- Fisher, R. A. (1992). Statistical methods for research workers. In *Breakthroughs in statistics*, pp. 66–70. Springer.
- Gamazon, E. R., H. E. Wheeler, K. P. Shah, S. V. Mozaffari, K. Aquino-Michaels, R. J.

- Carroll, A. E. Eyler, J. C. Denny, D. L. Nicolae, N. J. Cox, et al. (2015). A gene-based association method for mapping traits using reference transcriptome data. *Nature genetics* 47(9), 1091.
- Goldstein, J. L. and M. S. Brown (2009). The ldl receptor. *Arteriosclerosis, thrombosis, and vascular biology* 29(4), 431–438.
- Graham, S. E., S. L. Clarke, K.-H. H. Wu, S. Kanoni, G. J. Zajak, S. Ramdas, I. Surakka, I. Ntalla, S. Vedantam, T. W. Winkler, et al. (2021). The power of genetic diversity in genome-wide association studies of lipids. *Nature* 600(7890), 675–679.
- Grove, J., S. Ripke, T. D. Als, M. Mattheisen, R. K. Walters, H. Won, J. Pallesen, E. Agerbo, O. A. Andreassen, R. Anney, et al. (2019). Identification of common genetic risk variants for autism spectrum disorder. *Nature genetics* 51(3), 431–444.
- GTEx Consortium (2020). The gtex consortium atlas of genetic regulatory effects across human tissues. *Science* 369(6509), 1318–1330.
- GTEx Consortium, K. G. Ardlie, D. S. Deluca, A. V. Segrè, T. J. Sullivan, T. R. Young, E. T. Gelfand, C. A. Trowbridge, J. B. Maller, T. Tukiainen, et al. (2015). The genotype-tissue expression (gtex) pilot analysis: multitissue gene regulation in humans. *Science* 348(6235), 648–660.
- Gusev, A., A. Ko, H. Shi, G. Bhatia, W. Chung, B. W. Penninx, R. Jansen, E. J. De Geus, D. I. Boomsma, F. A. Wright, et al. (2016). Integrative approaches for large-scale transcriptome-wide association studies. *Nature genetics* 48(3), 245.
- Gutenbrunner, C. and J. Jurecková (1992). Regression rank scores and regression quantiles. *The Annals of Statistics*, 305–330.

- Gutenbrunner, C., J. Jurečková, R. Koenker, and S. Portnoy (1993). Tests of linear hypotheses based on regression rank scores. *Journaltitle of Nonparametric Statistics* 2(4), 307–331.
- Howard, D. M., M. J. Adams, T.-K. Clarke, J. D. Hafferty, J. Gibson, M. Shirali, J. R. Coleman, S. P. Hagenaars, J. Ward, E. M. Wigmore, et al. (2019). Genome-wide meta-analysis of depression identifies 102 independent variants and highlights the importance of the prefrontal brain regions. *Nature neuroscience* 22(3), 343–352.
- Hu, Y., M. Li, Q. Lu, H. Weng, J. Wang, S. M. Zekavat, Z. Yu, B. Li, J. Gu, S. Muchnik, et al. (2019). A statistical framework for cross-tissue transcriptome-wide association analysis. *bioRxiv*, 286013.
- Jansen, I. E., J. E. Savage, K. Watanabe, J. Bryois, D. M. Williams, S. Steinberg, J. Sealock, I. K. Karlsson, S. Hägg, L. Athanasiu, et al. (2019). Genome-wide meta-analysis identifies new loci and functional pathways influencing alzheimer’s disease risk. *Nature genetics* 51(3), 404–413.
- Jin, J. (2006). Higher criticism statistic: theory and applications in non-gaussian detection. In *Statistical Problems in Particle Physics, Astrophysics And Cosmology*, pp. 233–236. World Scientific.
- Koenker, R. and J. A. Machado (1999). Goodness of fit and related inference processes for quantile regression. *Journal of the american statistical association* 94(448), 1296–1310.
- Koenker, R. W. and G. Bassett (1978). Regression quantiles. *Econometrica* 46(1), 33–50.
- Kunkle, B. W., B. Grenier-Boley, R. Sims, J. C. Bis, V. Damotte, A. C. Naj, A. Boland, M. Vronskaya, S. J. Van Der Lee, A. Amlie-Wolf, et al. (2019). Genetic meta-analysis of

- diagnosed alzheimer’s disease identifies new risk loci and implicates α/β , tau, immunity and lipid processing. *Nature genetics* 51(3), 414–430.
- Leek, J. T. and J. D. Storey (2007). Capturing heterogeneity in gene expression studies by surrogate variable analysis. *PLoS genetics* 3(9), e161.
- Li, B., Y. Veturi, A. Verma, Y. Bradford, E. S. Daar, R. M. Gulick, S. A. Riddler, G. K. Robbins, J. L. Lennox, D. W. Haas, et al. (2021). Tissue specificity-aware twas (tsa-twas) framework identifies novel associations with metabolic, immunologic, and virologic traits in hiv-positive adults. *PLoS genetics* 17(4), e1009464.
- Li, D., Q. Liu, and P. S. Schnable (2021). Twas results are complementary to and less affected by linkage disequilibrium than gwas. *Plant physiology* 186(4), 1800–1811.
- Lin, Z., H. Xue, M. M. Malakhov, K. A. Knutson, and W. Pan (2022). Accounting for nonlinear effects of gene expression identifies additional associated genes in transcriptome-wide association studies. *Human molecular genetics*.
- Liu, Y. and J. Xie (2020). Cauchy combination test: a powerful test with analytic p-value calculation under arbitrary dependency structures. *Journal of the American Statistical Association* 115(529), 393–402.
- Ma, S., J. Dalglish, J. Lee, C. Wang, L. Liu, R. Gill, J. D. Buxbaum, W. K. Chung, H. Aschard, E. K. Silverman, et al. (2021). Powerful gene-based testing by integrating long-range chromatin interactions and knockoff genotypes. *Proceedings of the National Academy of Sciences* 118(47), e2105191118.
- Ma, S., C. Wang, A. Khan, L. Liu, J. Dalglish, K. Kiryluk, Z. He, and I. Ionita-Laza (2023).

- Bigknock: fine-mapping gene-based associations via knockoff analysis of biobank-scale data. *Genome Biology* 24(1), 24.
- Moscovich, A., B. Nadler, C. Spiegelman, et al. (2016). On the exact berk-jones statistics and their p -value calculation. *Electronic Journal of Statistics* 10(2), 2329–2354.
- Nagpal, S., X. Meng, M. P. Epstein, L. C. Tsoi, M. Patrick, G. Gibson, P. L. De Jager, D. A. Bennett, A. P. Wingo, T. S. Wingo, et al. (2019). Tigar: An improved bayesian tool for transcriptomic data imputation enhances gene mapping of complex traits. *The American Journal of Human Genetics* 105(2), 258–266.
- Nalls, M. A., C. Blauwendraat, C. L. Vallerga, K. Heilbron, S. Bandres-Ciga, D. Chang, M. Tan, D. A. Kia, A. J. Noyce, A. Xue, et al. (2019). Identification of novel risk loci, causal insights, and heritable risk for parkinson’s disease: a meta-analysis of genome-wide association studies. *The Lancet Neurology* 18(12), 1091–1102.
- O’Connor, L. J., A. Gusev, X. Liu, P.-R. Loh, H. K. Finucane, and A. L. Price (2017). Estimating the proportion of disease heritability mediated by gene expression levels. *BioRxiv*, 118018.
- Pan-UKB team (2020). <https://pan.ukbb.broadinstitute.org>.
- Pardiñas, A. F., P. Holmans, A. J. Pocklington, V. Escott-Price, S. Ripke, N. Carrera, S. E. Legge, S. Bishop, D. Cameron, M. L. Hamshire, et al. (2018). Common schizophrenia alleles are enriched in mutation-intolerant genes and in regions under strong background selection. *Nature genetics* 50(3), 381–389.
- Pierce, B. L., L. Tong, L. S. Chen, R. Rahaman, M. Argos, F. Jasmine, S. Roy, R. Paul-Brutus, H.-J. Westra, L. Franke, et al. (2014). Mediation analysis demonstrates that

- trans-eqtls are often explained by cis-mediation: a genome-wide analysis among 1,800 south asians. *PLoS genetics* 10(12), e1004818.
- PredictDB Team (2021). Gtex v8 models on eqtl and sqtl. </post/2021/07/21/gtex-v8-models-on-eqtl-and-sqtl/>.
- Somel, M., P. Khaitovich, S. Bahn, S. Pääbo, and M. Lachmann (2006). Gene expression becomes heterogeneous with age. *Current Biology* 16(10), R359–R360.
- Song, X., G. Li, Z. Zhou, X. Wang, I. Ionita-Laza, and Y. Wei (2017). Qrank: a novel quantile regression tool for eqtl discovery. *Bioinformatics* 33(14), 2123–2130.
- Stahl, E. A., G. Breen, A. J. Forstner, A. McQuillin, S. Ripke, V. Trubetskoy, M. Mattheisen, Y. Wang, J. R. Coleman, H. A. Gaspar, et al. (2019). Genome-wide association study identifies 30 loci associated with bipolar disorder. *Nature genetics* 51(5), 793–803.
- Stegle, O., L. Parts, R. Durbin, and J. Winn (2010). A bayesian framework to account for complex non-genetic factors in gene expression levels greatly increases power in eqtl studies. *PLoS computational biology* 6(5), e1000770.
- Stegle, O., L. Parts, M. Piipari, J. Winn, and R. Durbin (2012). Using probabilistic estimation of expression residuals (peer) to obtain increased power and interpretability of gene expression analyses. *Nature protocols* 7(3), 500–507.
- Sun, R., S. Hui, G. D. Bader, X. Lin, and P. Kraft (2019). Powerful gene set analysis in gwas with the generalized berk-jones statistic. *PLoS genetics* 15(3), e1007530.
- Tang, S., A. S. Buchman, P. L. De Jager, D. A. Bennett, M. P. Epstein, and J. Yang

- (2021). Novel variance-component twas method for studying complex human diseases with applications to alzheimer’s dementia. *PLoS genetics* 17(4), e1009482.
- Umans, B. D., A. Battle, and Y. Gilad (2021). Where are the disease-associated eqtls? *Trends in Genetics* 37(2), 109–124.
- Van Rheenen, W., A. Shatunov, A. M. Dekker, R. L. McLaughlin, F. P. Diekstra, S. L. Pulit, R. A. Van Der Spek, U. Vösa, S. De Jong, M. R. Robinson, et al. (2016). Genome-wide association analyses identify new risk variants and the genetic architecture of amyotrophic lateral sclerosis. *Nature genetics* 48(9), 1043–1048.
- Wainberg, M., N. Sinnott-Armstrong, N. Mancuso, A. N. Barbeira, D. A. Knowles, D. Golan, R. Ermel, A. Ruusalepp, T. Quertermous, K. Hao, et al. (2019). Opportunities and challenges for transcriptome-wide association studies. *Nature genetics* 51(4), 592–599.
- Wainberg, M., N. Sinnott-Armstrong, N. Mancuso, A. N. Barbeira, D. A. Knowles, D. Golan, R. Ermel, A. Ruusalepp, T. Quertermous, K. Hao, J. L. M. Björkegren, H. K. Im, B. Pasaniuc, M. A. Rivas, and A. Kundaje (2019). Opportunities and challenges for transcriptome-wide association studies. *Nature Genetics* 51(4), 592–599.
- Wang, C., Q. Tao, X. Wang, X. Wang, and X. Zhang (2016). Impact of high-fat diet on liver genes expression profiles in mice model of nonalcoholic fatty liver disease. *Environmental toxicology and pharmacology* 45, 52–62.
- Wang, C., T. Wang, Y. Wei, H. Aschard, and I. Ionita-Laza (2023). Quantile regression for biomarkers in the uk biobank. *bioRxiv*, 2023–06.
- Wang, H., F. Zhang, J. Zeng, Y. Wu, K. E. Kemper, A. Xue, M. Zhang, J. E. Powell,

- M. E. Goddard, N. R. Wray, et al. (2019). Genotype-by-environment interactions inferred from genetic effects on phenotypic variability in the uk biobank. *Science advances* 5(8), eaaw3538.
- Wang, T., I. Ionita-Laza, and Y. Wei (2022). Integrated quantile rank test (iqrat) for gene-level associations. *The Annals of Applied Statistics* 16(3), 1423–1444.
- Xie, Y., N. Shan, H. Zhao, and L. Hou. Transcriptome wide association studies: general framework and methods. *Quantitative Biology*, 0.
- Zhao, B., Y. Shan, Y. Yang, Z. Yu, T. Li, X. Wang, T. Luo, Z. Zhu, P. Sullivan, H. Zhao, et al. (2021). Transcriptome-wide association analysis of brain structures yields insights into pleiotropy with complex neuropsychiatric traits. *Nature communications* 12(1), 1–11.